ADVANCES IN ATMOSPHERIC SCIENCES, VOL. 37, JUNE 2020, 652–661

• **Original Paper** •

Relationship between Solar Wind−Magnetosphere Energy and Eurasian Winter Cold Events

Xinping XU*[1], Shengping HE[2,1], and Huijun WANG[1,3,4]

[1]*Collaborative Innovation Center on Forecast and Evaluation of Meteorological Disasters/Key Laboratory of Meteorological Disaster, Ministry of Education, Nanjing University of Information Science and Technology, Nanjing* 210044, *China*

[2]*Geophysical Institute, University of Bergen and Bjerknes Centre for Climate Research, Bergen* 5007, *Norway*

[3]*Nansen-Zhu International Research Center, Institute of Atmospheric Physics, Chinese Academy of Sciences, Beijing* 100029, *China*

[4]*Climate Change Research Center, Chinese Academy of Sciences, Beijing* 100029, *China*

(Received 15 July 2019; revised 7 February 2020; accepted 12 February 2020)

ABSTRACT

The profound impact of solar irradiance variations on the decadal variability of Earth's climate has been investigated by previous studies. However, it remains a challenge to quantify the energetic particle precipitation (EPP) influence on the surface climate, which is an emerging research topic. The solar wind is a source of magnetospheric EPP, and the total energy input from the solar wind into Earth's magnetosphere (E_{in}) shows remarkable interdecadal and interannual variability. Based on the new E_{in} index, this study reveals a significant interannual relationship between the annual mean E_{in} and Eurasian cold extremes in the subsequent winter. Less frequent cold events are observed over Eurasia (primarily north of 50°N) following the higher-than-normal E_{in} activity in the previous year, accompanied by more frequent cold events over northern Africa, and vice versa. This response pattern shows great resemblance to the first empirical orthogonal function of the variability of cold extremes over Eurasia, with a spatial correlation coefficient of 0.79. The pronounced intensification of the positive North Atlantic Oscillation events and poleward shift of the North Atlantic storm track associated with the anomalously higher E_{in} favor the anomalous extreme atmospheric circulation events, and thus less frequent extreme cold temperatures over northern Eurasia on the interannual time scale. It is further hypothesized that the wave−mean flow interaction in the stratosphere and troposphere is favorable for the connection of E_{in} signals to tropospheric circulation and climate in the following winter.

Key words: solar wind–magnetosphere energy, cold events, interannual variability, wave-mean flow interaction

Citation: Xu, X. P., S. P. He, and H. J. Wang, 2020: Relationship between solar wind−magnetosphere energy and Eurasian winter cold events. *Adv. Atmos. Sci.*, **37**(6), 652−661, https://doi.org/10.1007/s00376-020-9153-3.

Article Highlights:

- Significant interannual correlation is revealed between the annual mean E_{in} and Eurasian extreme cold events in the subsequent winter.
- A poleward shift of the North Atlantic storm track associated with E_{in} favors the anomalous circulation extremes.
- The wave−mean flow interaction in the stratosphere and troposphere is favorable for the connection of E_{in} to surface climate.

1. Introduction

Despite global climate warming, boreal winters have experienced frequent cold extremes with heavy snowfall in the early 21st century (Liu et al., 2012; Screen, 2014, 2015; Sun et al., 2016; Francis, 2017). Additionally, a remarkable surface cooling trend appears over Northern Hemisphere mid-latitudes after the late-1990s (Cohen et al., 2014; Kug et al., 2015). Many studies have explored possible reasons for such abnormal climate, such as Arctic sea-ice loss and Arctic warming (Honda et al., 2009; Mori et al., 2014; Wang and Liu, 2016; Screen, 2017b; Xu et al., 2018a, b, 2019) and internal atmospheric variability (Screen et al., 2014;

* Corresponding author: Xinping XU
Email: xuxinping1995@163.com

McCusker et al., 2016; Screen, 2017a; Ogawa et al., 2018). As the fundamental source of the climate system, solar activity has a profound impact on the decadal variability of boreal winter climate (Gray et al., 2010).

A mounting body of observational and modeling evidence converges on a common conclusion that the occurrence of European cold winters becomes high when the solar activity reaches its minimum on the decadal time scale (Lockwood et al., 2010; Woollings et al., 2010; Ineson et al., 2011; Matthes, 2011). The surface pressure pattern in response to the 11-year solar cycle projects onto the North Atlantic Oscillation (NAO) (Kodera, 2003; Thiéblemont et al., 2015), a dominant mode of the Northern Hemisphere atmospheric variability influencing winter weather and climate in the Eurasia–Atlantic sector (Wallace, 2000; Bader et al., 2011; Matthes, 2011; Cohen et al., 2014; Screen, 2017a). The physical link between the solar ultraviolet (UV) forcing and the decadal NAO variability has been suggested to arise from the "top-down" mechanism (Kodera and Kuroda, 2002; Gray et al., 2010). A lagged and amplified NAO response to the solar cycle is further proposed involving the ocean–atmosphere interaction mechanism (Gray et al., 2013; Scaife et al., 2013). Thiéblemont et al. (2015) revealed a 1–2-year lagged solar–NAO linkage via a multidecadal experiment with 11-year solar forcing variability. Sunspot number, open solar flux, and F10.7 cm radio flux, representing the decadal solar variability or solar UV variations, have been widely used to investigate the solar contribution to Earth's climate on the decadal time scale (Roy and Haigh, 2010; Woollings et al., 2010; Thiéblemont et al., 2015; Miao et al., 2018). However, the potential connections on the interannual time scale remain unclear.

In addition to radiative forcing, another important aspect of the solar activity influencing Earth's climate is energetic particle forcing (Lilensten et al., 2015). Matthes et al. (2017) recently suggested that changes in solar spectral irradiance (most importantly in the UV) and energetic particle precipitation (EPP) are two major players for the climate from the aspect of solar variability. The EPP consists of particles originating from the sun, Earth's magnetospheric field, and from beyond the solar system. Changes in EPP can lead to the production of NO_x through ionization and dissociation and the subsequent intricate chemical processes in the middle atmosphere (Jackman et al., 2006; Rozanov et al., 2012). Then, the polar winter descent of EPP-generated NO_x into the stratosphere affects the ozone abundance (Baumgaertner et al., 2011; Matthes et al., 2017). Sinnhuber et al. (2018) suggested that stratospheric EPP signals are more likely a result of dynamic processes than caused by downward descent of EPP-induced chemistry from the mesosphere and lower thermosphere. Rozanov et al. (2005) provided evidence that EPP-generated variations in stratospheric and tropospheric temperatures are comparable to those caused by solar UV forcing. The possible mechanisms linking the influence of EPP on the stratosphere to the surface are further suggested to be similar to those related to solar UV influence, including the accelerated stratospheric polar night jet and top-down coupling (Seppälä and Clilverd, 2014). Cnossen et al. (2016) also discussed the possible mechanism of downward connection from the thermosphere to the troposphere. However, a modeling study found that the EPP effect on tropospheric temperature is small and insignificant (Meraner and Schmidt, 2018).

As reviewed by Matthes et al. (2017), the influence of different EPP components on the surface climate is an emerging research topic, the challenge of which, however, is to quantify its climate impact. The solar wind, which cannot penetrate into the lower atmosphere directly but can violently interact with Earth's magnetosphere, serves as a source of EPP (Mironova et al., 2015). The solar wind resembles the high-speed stream generated from the solar coronal region-and mainly encompass electrons, protons, and α-particles. Lu et al. (2008) found a significant relationship between the solar wind and the Northern Annular Mode. The energy input from the solar wind into Earth's magnetosphere can cause space weather phenomena, such as magnetic storms, aurora, and so on (Akasofu, 1981). Magnetospheric particle precipitation associated with high-speed solar wind streams is more frequent during the decaying phase and near the minimum of the solar cycle (Sinnhuber et al., 2012).

Early studies suggest that the solar wind energy input is largely determined by the solar wind velocity (Crooker et al., 1977) or by the interplanetary magnetic field (IMF) (Dungey, 1961). Different opinions have been proposed since, but it remains a big challenge to quantitatively estimate the solar wind energy input into Earth's magnetosphere (E_{in}) (Akasofu, 1981; Newell et al., 2008). Recently, Wang et al. (2014) quantified E_{in} as a function of interplanetary and solar wind conditions, using three-dimensional magnetohydrodynamics. The new E_{in} index shows both quasi-decadal variability and interannual variability (He et al., 2018, 2019b), which provides a direct motivation for us to explore the potential interannual connections between the solar activity–controlled magnetospheric energetic particle forcing and the surface climate. Furthermore, He et al. (2018) revealed for the first time that E_{in} has a tangible effect on the interannual variability of the subsequent winter ENSO. With this in mind, is it plausible that the year-to-year variability of Eurasian winter weather and climate is linked to the solar wind energy penetrating Earth's magnetosphere. Thus, in this study, we attempt to understand the implications of the preceding E_{in} for winter extreme cold temperatures over Eurasia on the interannual time scale.

2. Data and methods

E_{in} (units: W) is estimated by a three-dimensional magnetohydrodynamic simulation (Wang et al., 2014),

$$E_{\text{in}} = 3.78\times 10^7 n_{\text{SW}}^{0.24} V_{\text{SW}}^{1.47} B_{\text{T}}^{0.86}\left[\sin^{2.70}\left(\frac{\theta}{2}\right)+0.25\right], \quad (1)$$

where n_{SW} (units: cm^{-3}) is the solar wind number density;

V_{SW} (units: km s^{-1}) is the solar wind velocity; B_T (units: nT) is the transverse magnetic field magnitude; θ is the IMF clock angle; and the solar wind data can be taken from the NASA OMNI project since 1963 (http://omniweb.gsfc.nasa.gov/). The energy input is more sensitive to the solar wind velocity and the IMF clock angle than other parameters (Wang et al., 2014). The monthly E_{in} is derived from the daily E_{in}. The annual mean E_{in} is employed to show the cumulative effect of energy input from the solar wind into Earth's magnetosphere. The annual mean E_{in} index is normalized. In the composite analysis, the higher (lower) E_{in} years are defined when the normalized annual mean E_{in} index is equal to or greater (less) than 0.5 (−0.5) standard deviation (Fig. 1c).

Daily surface air temperature (SAT) and atmospheric circulation data are derived from the NCEP−NCAR Reanalysis 1 with a horizontal resolution of 2.5° × 2.5° (Kalnay et al., 1996). The daily NAO indices are obtained from the Climate Prediction Center of NOAA (http://www.cpc.ncep.noaa.gov/products/precip/CWlink/pna/nao.shtml). In this paper, we focus on the winters of 1964−2018 considering the time range of the available E_{in} data. The winter of 1964 (for example) refers to December in 1964 and January and February in 1965. The relationship between E_{in} activity and winter cold events at lag +1 year (for example, the annual mean E_{in} in 1963 and cold events in winter 1964) is analyzed. All data are detrended before the regression, composite, and correlation analyses. The significance test is based on the standard two-tailed Student's t-test. The effective degree of freedom is computed as

$$N_e = N\frac{1-r_1 r_2}{1+r_1 r_2}\,, \tag{2}$$

where N is the number of samples; r_1 and r_2 are the autocorrelation coefficients of the two variables at one time interval (Bretherton et al., 1999).

Cold events are defined when the daily SAT is below the climatological mean SAT by 1.5 or more standard deviation (Thompson and Wallace, 2001). This study focuses on the total number of cold events in winter, as well as the number of extreme circulation events. Changes in extreme circulation events may not be simply identical to changes in the mean climate and are of greater concern to the public (Screen, 2017a). The extreme sea level pressure (SLP) events, 850-hPa wind (UV850; cyclone) events, and 300-hPa zonal wind (U300) events, are defined as the daily SLP/UV850/U300 above its 90th percentile (Pfahl, 2014). The negative (positive) NAO events are defined as intervals in which the normalized daily NAO index is lesser (greater) than or equal to −1.0 (+1.0) standard deviation for at least three consecutive days (Yao and Luo, 2015). Based on this definition, the frequency of negative (positive) NAO events in a winter is obtained by summing the duration of all negative (positive) NAO events in that winter. The 3−8-day bandpass-filtered 300-hPa transient eddies (v'^2) are calculated according to Murakami (1979).

We use the Eliassen−Palm (EP) flux ($\boldsymbol{F}$) and its divergence (D_F), which are calculated according to Edmon et al. (1980), to diagnose the wave−mean flow interaction (Andrews et al., 1987):

$$F(\varphi) = -\rho r_0 \cos\varphi \overline{u'v'}\,, \tag{3}$$

$$F(p) = \rho r_0 \cos\varphi \frac{\overline{\theta' v'}}{\overline{\theta_p}}\,, \tag{4}$$

$$D_F = \frac{\nabla\cdot\boldsymbol{F}}{\rho r_0 \cos\varphi}\,, \tag{5}$$

where ρ is the air density; r_0 is the radius of Earth; φ is the latitude; u and v are the zonal and meridional wind, respectively; θ is the potential temperature; p is the pressure, $\theta_p = d\theta/dp$; primes denote zonal deviations; and overbars denote zonal average. To display the EP flux throughout the stratosphere, the vectors are scaled by $\sqrt{1000/p}$ and $1/\rho$ (Wang et al., 2009). The vertical component is multiplied by 125 (Castanheira and Graf, 2003). An equatorward (upward) EP flux vector corresponds to a poleward eddy momentum (heat) flux, and the zonal-mean zonal flow decelerates (accelerates) where the EP flux converges (diverges) (Hartmann et al., 2000).

3. Results

3.1. *Interannual relationship between E_{in} and subsequent winter Eurasian cold extremes*

The frequency of Eurasian cold events in the subsequent winter regressed onto the annual mean E_{in} index is firstly presented in Fig. 1a. Clearly, there is a significantly decreased frequency of cold extremes over northern Asia, Russia and northern Scandinavia, primarily north of 50°N, and an increased frequency over northern Africa and near the Black and Caspian seas (Fig. 1a). The relationship between E_{in} activity and winter cold events at lag 0 or +2 years is weaker and less significant (Fig. 2). To further investigate the linkage between E_{in} and the interannual variability of extreme cold weather in the subsequent winter, the dominant interannual modes of cold events over Eurasia (20°−80°N, 0°−150°E) during 1964−2018 are extracted by performing empirical orthogonal function (EOF) analysis. The first mode of EOF (EOF1) explains 23.8% of the total variance, which is 8.6% larger than the second mode. The corresponding principal component of the EOF1 mode (PC1) shows remarkable interdecadal and interannual variability (figure not shown). EOF1 exhibits consistent negative values across the northern Eurasian continent and positive values in northern Africa (Fig. 1b). This pattern of cold events is quite similar to that following higher E_{in} in the preceding year, with a high spatial correlation coefficient of 0.79. The regions that cover (45°−70°N, 40°−140°E) and (20°−45°N, 0°−50°E) (red and blue rectangles in Figs. 1a and b) are hereafter referred to as northern Eurasia (NE) and northern

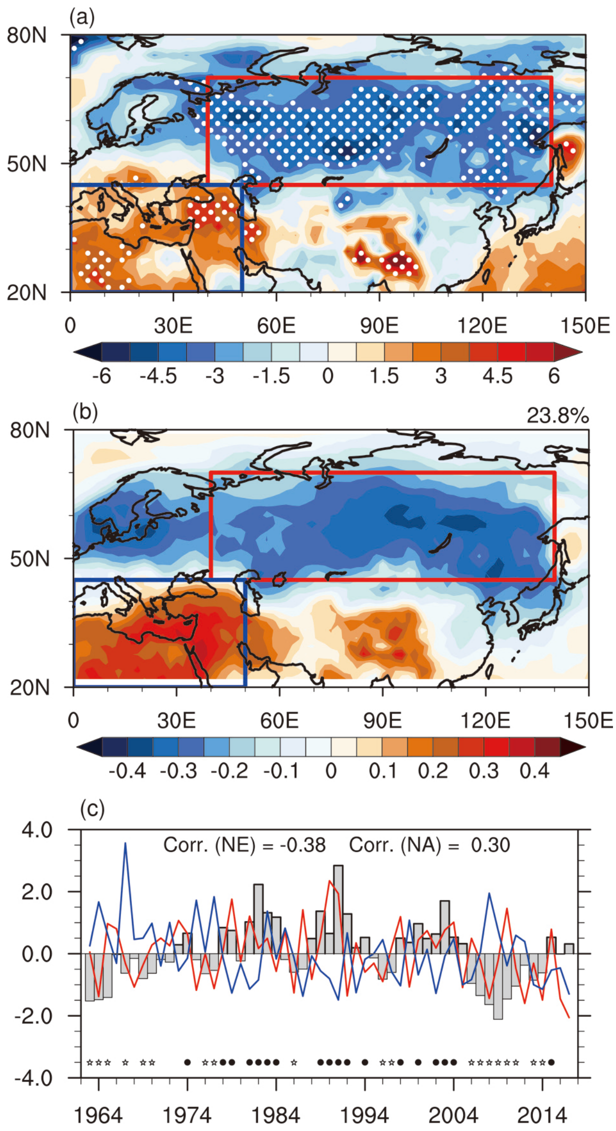

Fig. 1. (a) Regressions of frequency (units: d) of winter cold events during 1964–2018 against the normalized annual mean $E_{\rm in}$ index during 1963–2017. Dotted values are significant at the 95% confidence level based on the Student's *t*-test. (b) First mode of the EOF analysis for the frequency of winter cold events over Eurasia (20°–80°N, 0°–150°E) during 1964–2018. Red and blue boxes in (a) and (b) mark the regions where northern Eurasia (NE: 45°–70°N, 40°–140°E) and northern Africa (NA: 20°–45°N, 0°–40°E) are defined, respectively. (c) Normalized annual mean $E_{\rm in}$ index during 1963–2017 (bars) and normalized frequency of winter cold events during 1964–2018 over NE (blue lines) and NA (red lines). The dots (stars) indicate those years when the annual mean $E_{\rm in}$ index is equal to or greater (less) than 0.5 (−0.5) standard deviation. The correlation coefficients between the annual mean $E_{\rm in}$ index and frequency of winter cold events over NE and NA are given at the top of the panel.

Africa (NA), respectively. The linear correlation between the annual mean $E_{\rm in}$ index and the frequency of cold events over NE and NA are −0.38 and 0.30, respectively, significant at the 99% confidence level (Fig. 1c). Moreover, the probability for northern Eurasian winter to experience more than

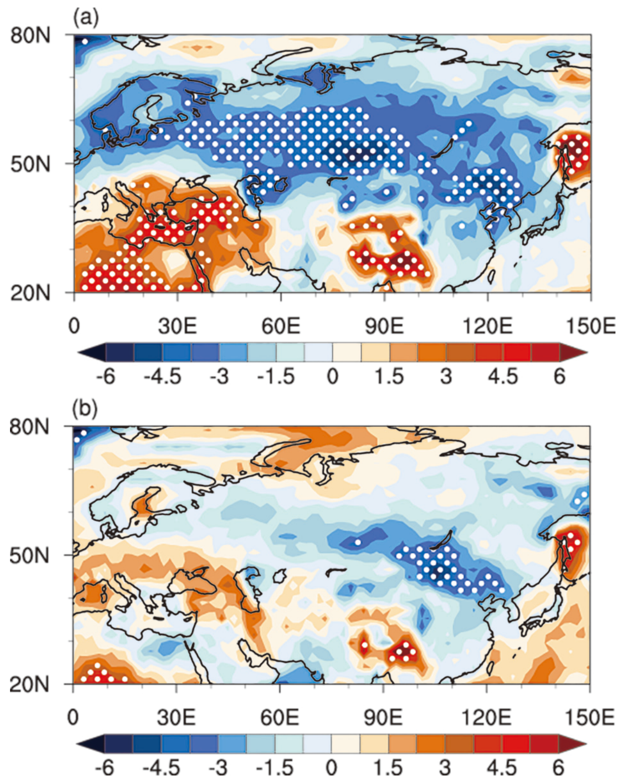

Fig. 2. Regressions of the frequency (units: d) of winter cold events during (a) 1963–2016 and (b) 1965–2018 against the normalized annual mean $E_{\rm in}$ index during 1963–2016. Dotted values are significant at the 95% confidence level based on the Student's *t*-test.

30 extreme cold days following a higher (lower) $E_{\rm in}$ year is about 26.7% (48.2%), based on the probability density function (PDF) of the occurrence of cold extremes; the PDF for cold days in NA at lag +1 year shows more occurrences of more than 30 extreme cold days (from 33.0% to 49.4%), in response to higher $E_{\rm in}$ relative to lower $E_{\rm in}$ (figure not shown). It is thus hypothesized that the magnetospheric particle precipitation from solar wind is associated with the interannual variations of Eurasian cold events in the subsequent winter.

3.2. *Extreme circulation events related to E_{in} variations*

Extreme cold temperatures over Eurasia are affected by anomalous circulations that are related to various forcing (Liu et al., 2012; Cohen et al., 2014). Figure 3a shows a decrease in the frequency of SLP extremes associated with PC1 in the Arctic region and a pronounced increase in the frequency at midlatitudes of the Europe–Atlantic sector (Fig. 3a). More frequent days with the lower-level anomalous anticyclone appear at midlatitudes (Fig. 3b). In the upper troposphere, more (less) frequent extreme strong westerly wind is shown to the north (south) of the climatological westerly jet (Fig. 3c), consistent with the significant positive (negative) U300 anomalies in the north of 50°N (south of 40°N) (figure not shown). This suggests the poleward shift of the North Atlantic westerly jet. The more (less) frequent strong westerly wind near the Norwegian (Mediterranean) Sea would drive milder (colder) conditions in NE (NA). Clearly, the anomalous circulation extremes related to the higher-than-normal E_{in} in the preceding year (Figs. 3d–f) are qualitatively in good agreement with those related to PC1 (Figs. 3a–c). This provides further support for the interannual connections between the solar wind–magnetosphere energy flux, the subsequent winter circulation extremes in the Europe–Atlantic sector, and extreme temperatures over Eurasia.

The North Atlantic synoptic-scale eddy variations play an important role in the highly variable midlatitude weather patterns (Cohen et al., 2014). Figure 4 presents the anomalous storm-track activity response to PC1 and the preceding annual mean E_{in}, separately. As expected, significantly enhanced storm-track activity emerges primarily in the high-latitude North Atlantic (Fig. 4). Previous studies have suggested that positive storm-track activity anomalies are intimately linked to westerly wind anomalies in situ, cyclonic eddy forcing to the north, and anticyclonic eddy forcing to the south (Lau, 1988; Gong et al., 2011; He et al., 2019a). The northward shift of the synoptic-scale eddies favors the northward shift of the North Atlantic westerly jet and more frequent strong westerly wind at high latitudes (Figs. 3c and f). The increases in the strength of the synoptic-scale eddy forcing at high latitudes are also tied to the cyclone extremes to the north and anticyclone extremes to the south (Figs. 3b and e). Considering the wider literature, changes in the North Atlantic storm tracks are consistent with the shift of the NAO phase (Bader et al., 2011; Cohen et al., 2014). A poleward shift of the storm track occurs when the NAO is in its positive phase (NAO|+) and an equatorward shift is observed in negative NAO (NAO|−) winters. The influence of geomagnetic activity on the NAO has been examined in previous studies (Baumgaertner et al., 2011; Li et al., 2011). A dynamical change of the positive shift of the NAO is thus expected in association with the higher solar

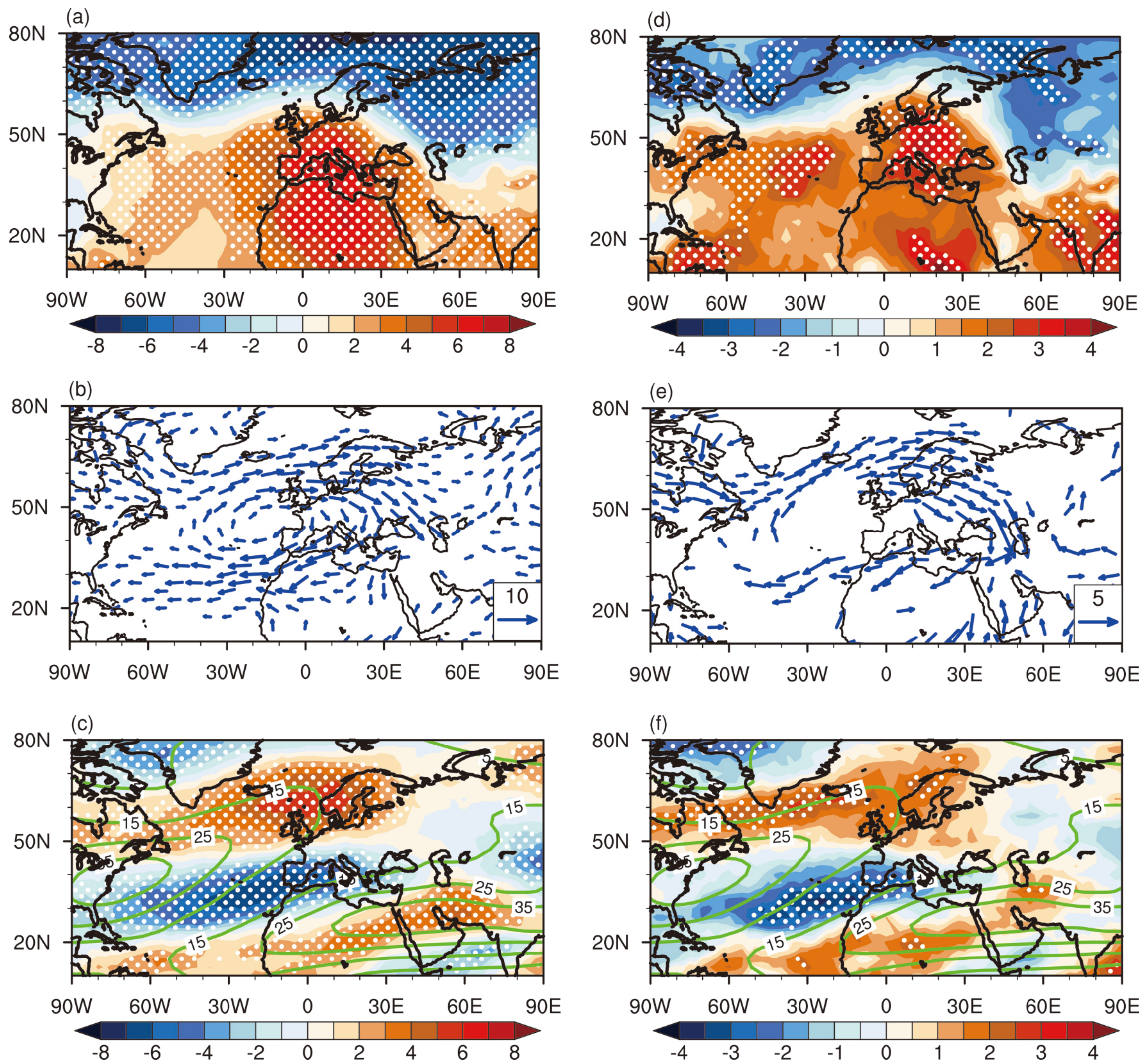

Fig. 3. (a–c) Regressions of the frequency (units: d) of winter (a) SLP, (b) UV850, and (c) U300 extremes during 1964–2018 against the normalized PC1 during 1964–2018. (d–f) As in (a–c), but regressed against the normalized annual mean E_{in} index during 1963–2017. (c, f) Green lines represent the climatology of winter U300 during 1964–2018. Vectors and dotted values are significant at the 95% confidence level based on the Student's t-test.

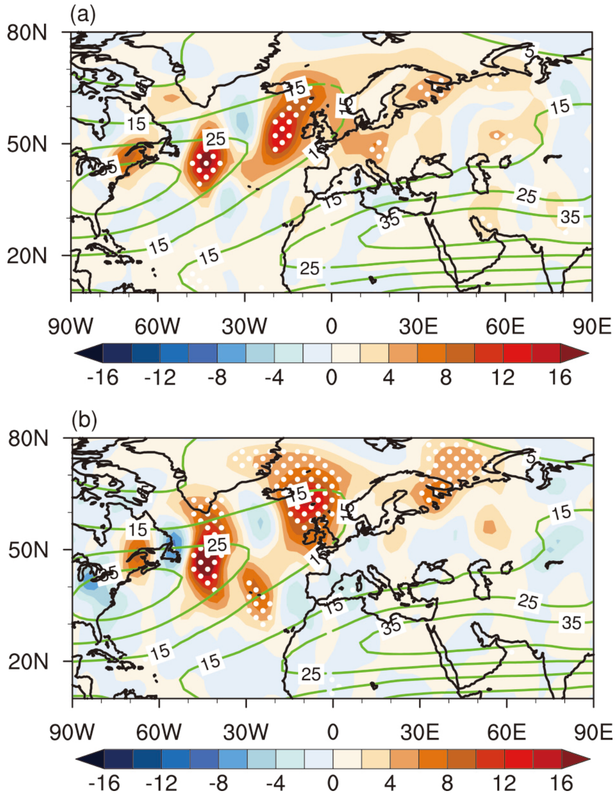

Fig. 4. Regressions of winter 3–8-day bandpass-filtered 300-hPa transient eddies (v'^2; units: 10^{-3} m^2 s^{-2}) against (a) the normalized PC1 during 1964–2018 and (b) the normalized annual mean $E_{\rm in}$ index during 1963–2017. Green lines represent the climatology of winter U300 during 1964–2018. Dotted values are significant at the 95% confidence level based on the Student's *t*-test.

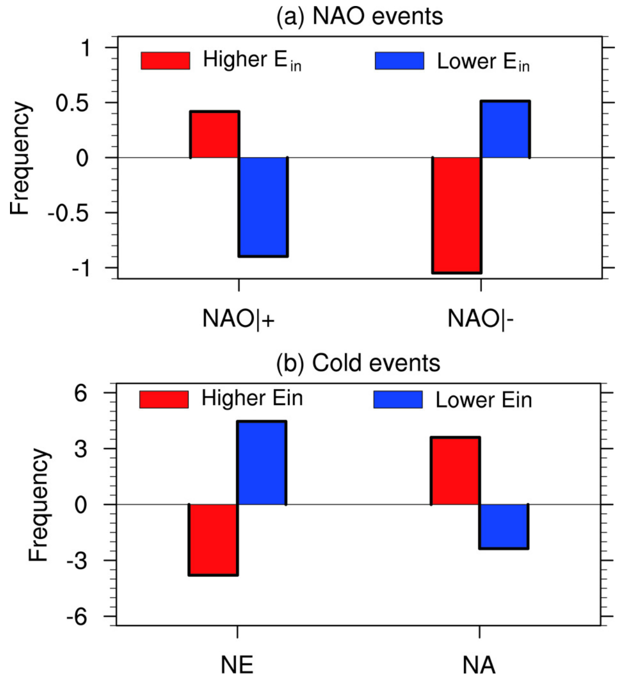

Fig. 5. Composites of the frequency of winter (a) NAO|+ and NAO|– events and (b) cold events over northern Eurasia (NE) and northern Africa (NA) during 1964–2018 following the higher (red bars) and lower (blue bars) $E_{\rm in}$ years during 1963–2017.

wind–magnetosphere energy flux input.

Next, we turn our attention to the frequency of strong NAO events following higher and lower $E_{\rm in}$ years. As shown in Fig. 5a, the composite occurrence of 1-year-lagged NAO|+ events is higher-than-normal following higher $E_{\rm in}$, and lower-than-normal following lower $E_{\rm in}$. Similarly, the NAO|– events have a higher frequency following lower $E_{\rm in}$ compared to higher $E_{\rm in}$ (Fig. 5a). These differences support the notion that the subsequent winter NAO|+ (NAO|–) events are intensified (weakened) following higher $E_{\rm in}$ activity, favoring less frequent cold events in NE and more frequent cold events in NA, and vice versa (Fig. 5b).

4. Discussion on the mechanism

The potential influence of magnetospheric energetic particle forcing on stratospheric circulation has been suggested in previous studies (Seppälä et al., 2009; Baumgaertner et al., 2011; Rozanov et al., 2012). Associated with the higher energy input from the solar wind into Earth's magnetosphere, the tropical region warms in the upper troposphere and lower stratosphere in the following year from spring (March–May) to winter (Fig. 6a). This might be due to the cumulative effect of energy input from the solar wind into Earth's magnetosphere and increased ozone heating (Kodera and Kuroda, 2002; Cionni et al., 2011). Additionally, it is also possible that the relationship between $E_{\rm in}$ and equatorial temperature is modulated by ENSO, because a previous study revealed a close relationship between boreal winter ENSO and the preceding annual-mean solar wind–magnetosphere energy flux input (He et al., 2018). The westerly wind is profoundly accelerated throughout the troposphere and stratosphere in boreal winter (Fig. 6b), which might be attributable to the intensified northward temperature gradient due to the persistent warming at lower latitudes (Fig. 6a). There are anomalous downward-pointing EP flux vectors from the stratosphere to the upper troposphere in the following December and January (Figs. 7a and b; vectors), suggesting reduced upward Rossby wave propagation from the troposphere into the stratosphere. Also, the EP flux divergent anomalies in the troposphere (Figs. 7a and b; contours) are consistent with westerly anomalies at 20°–35°N and 50°–75°N and easterly anomalies in between (Fig. 3f). This wave–mean flow interaction (Charney and Drazin, 1961; Hartmann et al., 2000) is favorable for maintaining the downward propagation of the solar signals (Thiéblemont et al., 2015) and the connection of $E_{\rm in}$ signals to tropospheric circulation and climate. It might be the case that there is no clear wave–mean flow interaction associated with $E_{\rm in}$ in February (Fig. 7c). However, there are some significant SLP anomalies in February (Fig. 8c), consistent with those in December and January (Figs. 8a and b). This might be because the impacts of $E_{\rm in}$ have propagated into the troposphere in December and January (Figs. 7a and b).

5. Conclusion

Solar activity is a major energy source of Earth's climate, through changes in radiative forcing and energetic particle forcing (Lilensten et al., 2015). The impacts of the variation in solar irradiance on the decadal variability of Eurasian winter climate have been well recorded in the literature (Gray et al., 2010; Woollings et al., 2010; Thiéblemont

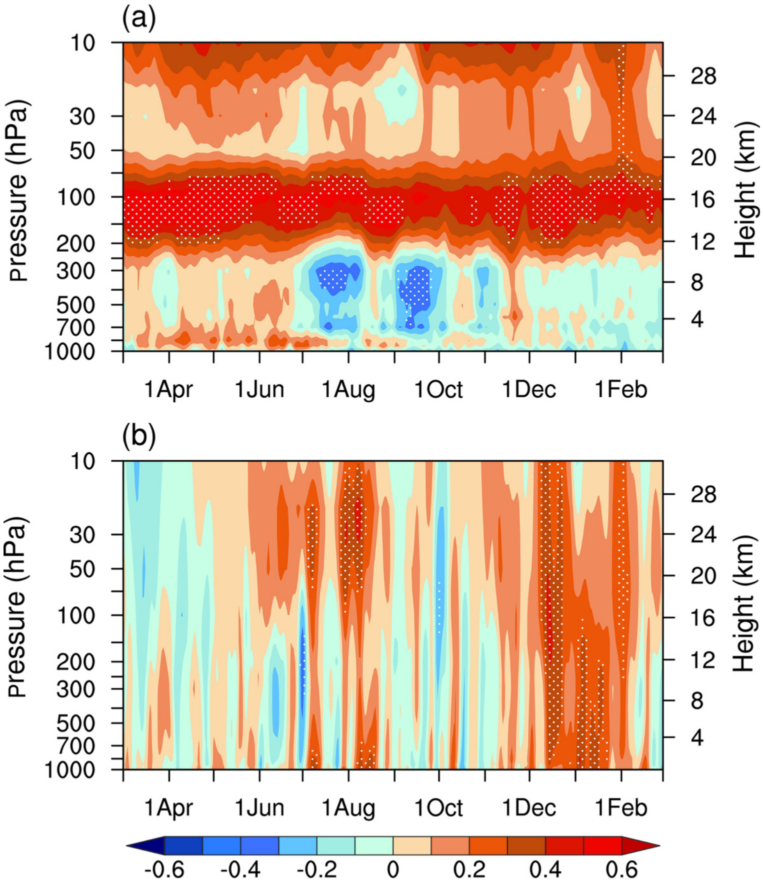

Fig. 6. Vertical−horizontal cross section for the correlations between the daily zonal-mean (a) temperature averaged along 30°S−30°N and (b) zonal wind averaged along 55°−65°N (from 1 March to 28 February, with 5-day low-pass filtering) during 1964/65−2018/19 and the normalized annual mean E_{in} index during 1963−2017. Dotted values are significant at the 95% confidence level based on the Student's *t*-test. The effective degrees of freedom are adopted in (a) for the Student's *t*-test.

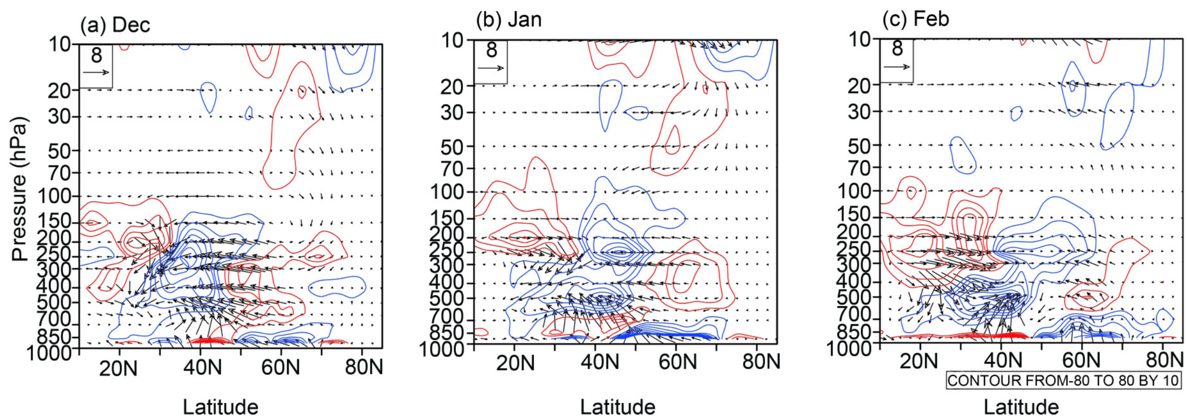

Fig. 7. Composites of the subsequent (a) December, (b) January, and (c) February Eliassen−Palm flux (vectors; units: 10^7 m^2 s^{-2}) and its divergence anomalies (contours; units: m s^{-1} d^{-1}; red/blue contours indicate anomalous divergence/convergence) between the higher and lower E_{in} years during 1963−2017.

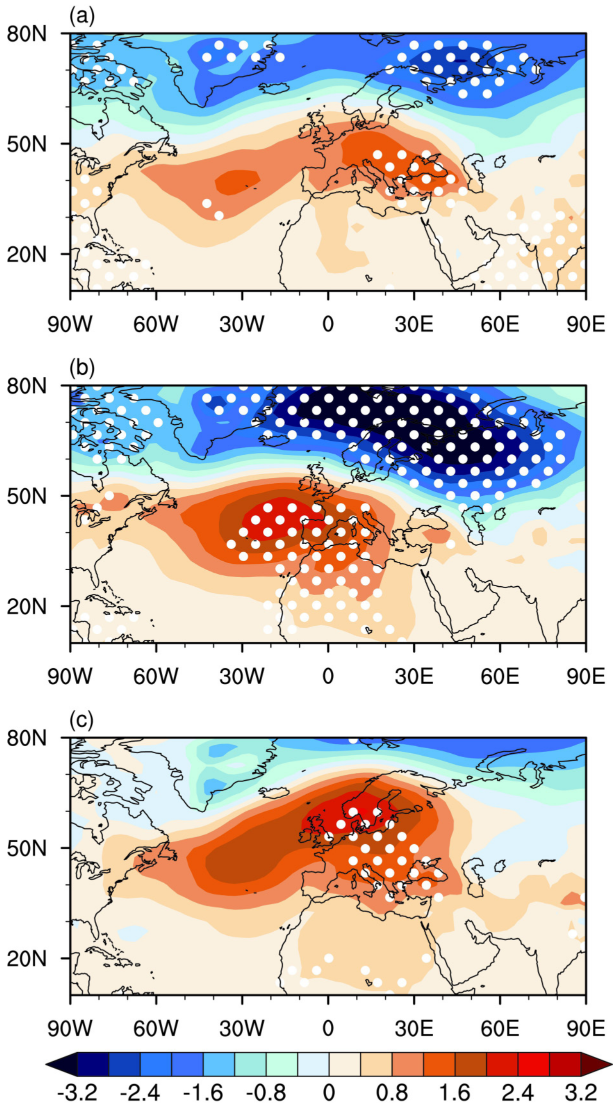

Fig. 8. Regressions of the subsequent (a) December, (b) January, and (c) February frequency (units: d) of SLP extremes during 1964/65–2018/19 against the normalized annual mean $E_{\rm in}$ index during 1963–2017. Dotted values are significant at the 95% confidence level based on the Student's *t*-test.

et al., 2015). However, it remains a big challenge to quantify the influence of the different EPP components on the surface climate, which is an emerging research topic (Matthes et al., 2017).

The solar wind serves as a source of magnetospheric energetic particle forcing, in the main form of electrons (Mironova et al., 2015). Recently, Wang et al. (2014) quantified the solar wind energy input into Earth's magnetosphere ($E_{\rm in}$) using three-dimensional magnetohydrodynamics. It is worth noting that this new $E_{\rm in}$ index exhibits both interdecadal and interannual variability (He et al., 2018, 2019b). The interannual relationship between the solar wind energy penetrating Earth's magnetosphere and Eurasian cold extremes in the subsequent winter is thus explored in this study. The results show that the frequency of cold winter events following years with increased solar wind–magnetosphere energy flux shows a significant decrease over NE and increase in NA, and vice versa. This is broadly similar to the dominant EOF mode of interannual variability in Eurasian cold extremes, with a high spatial correlation coefficient of 0.79. The high variance of winter cold events over NE and NA explained by the preceding annual mean $E_{\rm in}$ can reach up to 0.2 (figure not shown). Moreover, the frequent positive NAO (NAO|+) events and poleward shift of the North Atlantic storm track activities following the preceding higher-than-normal $E_{\rm in}$ activity, favors the anomalous circulation extremes and less frequent extreme cold temperatures over northern Eurasia. It is further hypothesized that the wave–mean flow interaction in the stratosphere and troposphere is favorable for the connection of $E_{\rm in}$ signals to tropospheric circulation and climate in the following winter. In general, our study provides further insight into the potential interannual linkage between EPP variations and the surface extreme cold weather.

Acknowledgements. This work was supported by the National Key R&D Program of China (Grant No. 2016YFA0600703), the National Natural Science Foundation of China (Grant Nos. 41875118, 41605059 and 41505073), the Postgraduate Research & Practice Innovation Program of Jiangsu Province (Grant No. KYCX18_0997), the funding of the Jiangsu Innovation & Entrepreneurship Team, and the Priority Academic Program Development (PAPD) of Jiangsu Higher Education Institutions. This work was partially supported by the International Space Science Institute (ISSI) in Beijing, through the working team "Dynamical signatures of energetic particle precipitation in atmospheric re-analyses" (ID:32, 2019).

REFERENCES

Akasofu, S.-I., 1981: Energy coupling between the solar wind and the magnetosphere. *Space Science Reviews*, **28**, 121−190, https://doi.org/10.1007/BF00218810.

Andrews, D. G., J. R. Holton, and C. B. Leovy, 1987: *Middle Atmosphere Dynamics*. Academic Press, Cambridge, 489 pp.

Bader, J., M. D. S. Mesquita, K. I. Hodges, N. Keenlyside, S. Østerhus, and M. Miles, 2011: A review on Northern Hemisphere sea-ice, storminess and the North Atlantic Oscillation: Observations and projected changes. *Atmospheric Research*, **101**, 809−834, https://doi.org/10.1016/j.atmosres.2011.04.007.

Baumgaertner, A. J. G., A. Seppälä, P. Jöckel, and M. A. Clilverd, 2011: Geomagnetic activity related NOx enhancements and polar surface air temperature variability in a chemistry climate model: Modulation of the NAM index. *Atmospheric Chemistry and Physics*, **11**, 4521−4531, https://doi.org/10.5194/acp-11-4521-2011.

Bretherton, C. S., M. Widmann, V. P. Dymnikov, J. M. Wallace, and I. Bladé, 1999: The effective number of spatial degrees of freedom of a time-varying field. *J. Climate*, **12**, 1990−2009, https://doi.org/10.1175/1520-0442(1999)012<1990:TENOSD>2.0.CO;2.

Castanheira, J. M., and H.-F. Graf, 2003: North Pacific-North Atlantic relationships under stratospheric control? J *Geophys. Res.*, **108**, 4036, https://doi.org/10.1029/2002JD002754.

Charney, J. G., and P. G. Drazin, 1961: Propagation of planetary-scale disturbances from the lower into the upper atmosphere. *J. Geophys. Res.*, **66**, 83–109, https://doi.org/10.1029/JZ066i001p00083.

Cionni, I., and Coauthors, 2011: Ozone database in support of CMIP5 simulations: Results and corresponding radiative forcing. *Atmospheric Chemistry and Physics*, **11**, 11267–11292, https://doi.org/10.5194/acp-11-11267-2011.

Cnossen, I., H. L. Liu, and H. Lu, 2016: The whole atmosphere response to changes in the Earth's magnetic field from 1900 to 2000: An example of "top-down" vertical coupling. *J. Geophys. Res.*, **121**, 7781–7800, https://doi.org/10.1002/2016JD024890.

Cohen, J., and Coauthors, 2014: Recent Arctic amplification and extreme mid-latitude weather. *Nature Geoscience*, **7**, 627–637, https://doi.org/10.1038/ngeo2234.

Crooker, N. U., J. Feynman, and J. T. Gosling, 1977: High correlation between long-term averages of solar wind speed and geomagnetic activity. *J. Geophys. Res.*, **82**, 1933–1937, https://doi.org/10.1029/JA082i013p01933.

Dungey, J. W., 1961: Interplanetary magnetic field and the auroral zones. *Physical Review Letters*, **6**, 47–48, https://doi.org/10.1103/PhysRevLett.6.47.

Edmon, H. J., Jr., B. J. Hoskins, and M. E. McIntyre, 1980: Eliassen-Palm cross sections for the troposphere. *J. Atmos. Sci.*, **37**, 2600–2616, https://doi.org/10.1175/1520-0469(1980)037<2600:EPCSFT>2.0.CO;2.

Francis, J. A., 2017: Why are Arctic linkages to extreme weather still up in the air? *Bull. Amer. Meteorol. Soc.*, **98**, 2551–2557, https://doi.org/10.1175/BAMS-D-17-0006.1.

Gong, D.-Y., J. Yang, S.-J. Kim, Y. Q. Gao, D. Guo, T. J. Zhou, and M. Hu, 2011: Spring Arctic Oscillation-East Asian summer monsoon connection through circulation changes over the western North Pacific. *Climate Dyn.*, **37**, 2199–2216, https://doi.org/10.1007/s00382-011-1041-1.

Gray, L. J., and Coauthors, 2010: Solar influence on climate. *Rev. Geophys.*, **48**, RG4001, https://doi.org/10.1029/2009RG000282.

Gray, L. J., and Coauthors, 2013: A lagged response to the 11 year solar cycle in observed winter Atlantic/European weather patterns. *J. Geophys. Res.*, **118**, 13 405–13 420, https://doi.org/10.1002/2013JD020062.

Hartmann, D. L., J. M. Wallace, V. Limpasuvan, D. W. J. Thompson, and J. R. Holton, 2000: Can ozone depletion and global warming interact to produce rapid climate change? *Proceedings of the National Academy of Sciences of the United States of America*, **97**, 1412–1417, https://doi.org/10.1073/pnas.97.4.1412.

He, S.-P., H.-J. Wang, Y.-Q. Gao, F. Li, H. Li, and C. Wang, 2018: Influence of solar wind energy flux on the interannual variability of ENSO in the subsequent year. *Atmospheric and Oceanic Science Letters*, **11**, 165–172, https://doi.org/10.1080/16742834.2018.1436367.

He, S. P., H. J. Wang, Y. Q. Gao, and F. Li, 2019a: Recent intensified impact of December Arctic Oscillation on subsequent January temperature in Eurasia and North Africa. *Climate Dyn.*, **52**, 1077–1094, https://doi.org/10.1007/s00382-018-4182-7.

He, S. P., H. J. Wang, F. Li, H. Li, and C. Wang, 2019b: Solar-wind-magnetosphere energy influences the interannual variability of the northern-hemispheric winter climate. *National Science Review*, https://doi.org/10.1093/nsr/nwz082.

Honda, M., J. Inoue, and S. Yamane, 2009: Influence of low Arctic sea-ice minima on anomalously cold Eurasian winters. *Geophys. Res. Lett.*, **36**, L08707, https://doi.org/10.1029/2008GL037079.

Ineson, S., A. A. Scaife, J. R. Knight, J. C. Manners, N. J. Dunstone, L. J. Gray, and J. D. Haigh, 2011: Solar forcing of winter climate variability in the Northern Hemisphere. *Nature Geoscience*, **4**, 753–757, https://doi.org/10.1038/ngeo1282.

Jackman, C. H., M. T. Deland, G. J. Labow, E. L. Fleming, and M. López-Puertas, 2006: Satellite measurements of middle atmospheric impacts by solar proton events in Solar cycle 23. *Space Science Reviews*, **125**, 381–391, https://doi.org/10.1007/s11214-006-9071-4.

Kalnay, E., and Coauthors, 1996: The NCEP/NCAR 40-year reanalysis project. *Bull. Amer. Meteorol. Soc.*, **77**, 437–472, https://doi.org/10.1175/1520-0477(1996)077<0437:TNYRP>2.0.CO;2.

Kodera, K., 2003: Solar influence on the spatial structure of the NAO during the winter 1900-1999. *Geophys. Res. Lett.*, **30**, 1175, https://doi.org/10.1029/2002GL016584.

Kodera, K., and Y. Kuroda, 2002: Dynamical response to the solar cycle. *J. Geophys. Res.*, **107**, 4749, https://doi.org/10.1029/2002JD002224.

Kug, J.-S., J.-H. Jeong, Y.-S. Jang, B.-M. Kim, C. K. Folland, S.-K. Min, and S.-W. Son, 2015: Two distinct influences of Arctic warming on cold winters over North America and East Asia. *Nature Geoscience*, **8**, 759–762, https://doi.org/10.1038/ngeo2517.

Lau, N.-C., 1988: Variability of the observed midlatitude storm tracks in relation to low-frequency changes in the circulation pattern. *J. Atmos. Sci.*, **45**, 2718–2743, https://doi.org/10.1175/1520-0469(1988)045<2718:VOTOMS>2.0.CO;2.

Li, Y., H. Lu, M. J. Jarvis, M. A. Clilverd, and B. Bates, 2011: Nonlinear and nonstationary influences of geomagnetic activity on the winter North Atlantic Oscillation. *J. Geophys. Res.*, **116**, D16109, https://doi.org/10.1029/2011JD015822.

Lilensten, J., T. D. de Wit, and K. Matthes, 2015: *Earth's Climate Response to a Changing Sun*. EDP Sciences, Paris.

Liu, J. P., J. A. Curry, H. J. Wang, M. R. Song, and R. M. Horton, 2012: Impact of declining Arctic sea ice on winter snowfall. *Proceedings of the National Academy of Sciences of the United States of America*, **109**, 4074–4079, https://doi.org/10.1073/pnas.1114910109.

Lockwood, M., R. G. Harrison, T. Woollings, and S. K. Solanki, 2010: Are cold winters in Europe associated with low solar activity? *Environmental Research Letters*, **5**, 024001, https://doi.org/10.1088/1748-9326/5/2/024001.

Lu, H., M. J. Jarvis, and R. E. Hibbins, 2008: Possible solar wind effect on the Northern Annular Mode and northern hemispheric circulation during winter and spring. *J. Geophys. Res.*, **113**, D23104, https://doi.org/10.1029/2008JD010848.

Matthes, K., 2011: Atmospheric science: Solar cycle and climate predictions. *Nature Geoscience*, **4**, 735–736, https://doi.org/10.1038/ngeo1298.

Matthes, K., and Coauthors, 2017: Solar forcing for CMIP6 (v3.2). *Geoscientific Model Development*, **10**, 2247–2302, https://doi.org/10.5194/gmd-10-2247-2017.

McCusker, K. E., J. C. Fyfe, and M. Sigmond, 2016: Twenty-five winters of unexpected Eurasian cooling unlikely due to Arctic sea-ice loss. *Nature Geoscience*, **9**, 838–842, https://doi.org/10.1038/ngeo2820.

Meraner, K., and H. Schmidt, 2018: Climate impact of idealized winter polar mesospheric and stratospheric ozone losses as caused by energetic particle precipitation. *Atmospheric Chemistry and Physics*, **18**, 1079–1089, https://doi.org/10.5194/acp-18-1079-2018.

Miao, J. P., T. Wang, H. J. Wang, and Y. Q. Gao, 2018: Influence of low-frequency Solar forcing on the East Asian winter monsoon based on HadCM3 and observations. *Adv. Atmos. Sci.*, **35**, 1205−1215, https://doi.org/10.1007/s00376-018-7229-0.

Mironova, I. A., and Coauthors, 2015: Energetic particle influence on the Earth's atmosphere. *Space Science Reviews*, **194**, 1−96, https://doi.org/10.1007/s11214-015-0185-4.

Mori, M., M. Watanabe, H. Shiogama, J. Inoue, and M. Kimoto, 2014: Robust Arctic sea-ice influence on the frequent Eurasian cold winters in past decades. *Nature Geoscience*, **7**, 869−873, https://doi.org/10.1038/ngeo2277.

Murakami, M., 1979: Large-scale aspects of deep convective activity over the GATE area. *Mon. Wea. Rev.*, **107**, 994−1013, https://doi.org/10.1175/1520-0493(1979)107<0994:LSAODC>2.0.CO;2.

Newell, P. T., T. Sotirelis, K. Liou, and F. J. Rich, 2008: Pairs of solar wind-magnetosphere coupling functions: Combining a merging term with a viscous term works best. *J. Geophys. Res.*, **113**, A04218, https://doi.org/10.1029/2007JA012825.

Ogawa, F., and Coauthors, 2018: Evaluating impacts of recent Arctic sea ice loss on the northern hemisphere winter climate change. *Geophys. Res. Lett.*, **45**, 3255−3263, https://doi.org/10.1002/2017GL076502.

Pfahl, S., 2014: Characterising the relationship between weather extremes in Europe and synoptic circulation features. *Natural Hazards and Earth System Sciences*, **14**, 1461−1475, https://doi.org/10.5194/nhess-14-1461-2014.

Roy, I., and J. D. Haigh, 2010: Solar cycle signals in sea level pressure and sea surface temperature. *Atmospheric Chemistry and Physics*, **10**, 3147−3153, https://doi.org/10.5194/acp-10-3147-2010.

Rozanov, E., L. Callis, M. Schlesinger, F. Yang, N. Andronova, and V. Zubov, 2005: Atmospheric response to NOy source due to energetic electron precipitation. *Geophys. Res. Lett.*, **32**, L14811, https://doi.org/10.1029/2005GL023041.

Rozanov, E., M. Calisto, T. Egorova, T. Peter, and W. Schmutz, 2012: Influence of the precipitating energetic particles on atmospheric chemistry and climate. *Surveys in Geophysics*, **33**, 483−501, https://doi.org/10.1007/s10712-012-9192-0.

Scaife, A. A., S. Ineson, J. R. Knight, L. Gray, K. Kodera, and D. M. Smith, 2013: A mechanism for lagged North Atlantic climate response to solar variability. *Geophys. Res. Lett.*, **40**, 434−439, https://doi.org/10.1002/grl.50099.

Screen, J. A., 2014: Arctic amplification decreases temperature variance in northern mid- to high-latitudes. *Nat. Clim. Change*, **4**, 577−582, https://doi.org/10.1038/nclimate2268.

Screen, J. A., 2017a: The missing Northern European winter cooling response to Arctic sea ice loss. *Nature Communications*, **8**, 14603, https://doi.org/10.1038/ncomms14603.

Screen, J. A., 2017b: Far-flung effects of Arctic warming. *Nature Geoscience*, **10**, 253−254, https://doi.org/10.1038/ngeo2924.

Screen, J. A., C. Deser, I. Simmonds, and R. Tomas, 2014: Atmospheric impacts of Arctic sea-ice loss, 1979−2009: Separating forced change from atmospheric internal variability. *Climate Dyn.*, **43**, 333−344, https://doi.org/10.1007/s00382-013-1830-9.

Screen, J. A., C. Deser, and L. T. Sun, 2015: Reduced risk of North American cold extremes due to continued Arctic sea ice loss. *Bull. Amer. Meteorol. Soc.*, **96**, 1489−1503, https://doi.org/10.1175/BAMS-D-14-00185.1.

Seppälä, A., and M. A. Clilverd, 2014: Energetic particle forcing of the Northern Hemisphere winter stratosphere: Comparison to solar irradiance forcing. *Frontiers in Physics*, **2**, 25, https://doi.org/10.3389/fphy.2014.00025.

Seppälä, A., C. E. Randall, M. A. Clilverd, E. Rozanov, and C. J. Rodger, 2009: Geomagnetic activity and polar surface air temperature variability. *J. Geophys. Res.*, **114**, A10312, https://doi.org/10.1029/2008JA014029.

Sinnhuber, M., and Coauthors, 2018: NOy production, ozone loss and changes in net radiative heating due to energetic particle precipitation in 2002−2010. *Atmospheric Chemistry and Physics*, **18**, 1115−1147, https://doi.org/10.5194/acp-18-1115-2018.

Sinnhuber, M., H. Nieder, and N. Wieters, 2012: Energetic particle precipitation and the chemistry of the mesosphere/lower thermosphere. *Surveys in Geophysics*, **33**, 1281−1334, https://doi.org/10.1007/s10712-012-9201-3.

Sun, L. T., J. Perlwitz, and M. Hoerling, 2016: What caused the recent "warm Arctic, cold continents" trend pattern in winter temperatures? *Geophys. Res. Lett.*, **43**, 5345−5352, https://doi.org/10.1002/2016GL069024.

Thiéblemont, R., K. Matthes, N.-E. Omrani, K. Kodera, and F. Hansen, 2015: Solar forcing synchronizes decadal North Atlantic climate variability. *Nature Communications*, **6**, 8268, https://doi.org/10.1038/ncomms9268.

Thompson, D. W. J., and J. M. Wallace, 2001: Regional climate impacts of the Northern Hemisphere annular mode. *Science*, **293**, 85−89, https://doi.org/10.1126/science.1058958.

Wallace, J. M., 2000: North atlantic oscillatiodannular mode: Two paradigms-one phenomenon. *Quart. J. Roy. Meteorol. Soc.*, **126**, 791−805, https://doi.org/10.1002/qj.49712656402.

Wang, C., J. P. Han, H. Li, Z. Peng, and J. D. Richardson, 2014: Solar wind-magnetosphere energy coupling function fitting: Results from a global MHD simulation. *J. Geophys. Res.*, **119**, 6199−6212, https://doi.org/10.1002/2014JA019834.

Wang, L., R. H. Huang, L. Gu, W. Chen, and L. H. Kang, 2009: Interdecadal variations of the East Asian winter monsoon and their association with quasi-stationary planetary wave activity. *J. Climate*, **22**, 4860−4872, https://doi.org/10.1175/2009JCLI2973.1.

Wang, S.-Y., and J. P. Liu, 2016: Delving into the relationship between autumn Arctic sea ice and central-eastern Eurasian winter climate. *Atmospheric and Oceanic Science Letters*, **9**, 366−374, https://doi.org/10.1080/16742834.2016.1207482.

Woollings, T., M. Lockwood, G. Masato, C. Bell, and L. Gray, 2010: Enhanced signature of solar variability in Eurasian winter climate. *Geophys. Res. Lett.*, **37**, L20805, https://doi.org/10.1029/2010GL044601.

Xu, X. P., F. Li, S. P. He, and H. J. Wang, 2018a: Subseasonal reversal of East Asian surface temperature variability in winter 2014/15. *Adv. Atmos. Sci.*, **35**, 737−752, https://doi.org/10.1007/s00376-017-7059-5.

Xu, X. P., S. P. He, F. Li, and H. J. Wang, 2018b: Impact of northern Eurasian snow cover in autumn on the warm Arctic-cold Eurasia pattern during the following January and its linkage to stationary planetary waves. *Climate Dyn.*, **50**, 1993−2006, https://doi.org/10.1007/s00382-017-3732-8.

Xu, X. P., S. P. He, Y. Q. Gao, T. Furevik, H. J. Wang, F. Li, and F. Ogawa, 2019: Strengthened linkage between midlatitudes and Arctic in boreal winter. *Climate Dyn.*, **53**, 3971−3983, https://doi.org/10.1007/s00382-019-04764-7.

Yao, Y., and D. H. Luo, 2015: Do European blocking events precede North Atlantic Oscillation events? *Adv. Atmos. Sci.*, **32**, 1106−1118, https://doi.org/10.1007/s00376-015-4209-5.